



ALMA MATER STUDIORUM
UNIVERSITÀ DI BOLOGNA

ARCHIVIO ISTITUZIONALE
DELLA RICERCA

Alma Mater Studiorum Università di Bologna Archivio istituzionale della ricerca

Morpho-functional analyses reveal that changes in the chemical structure of a marine bisindole alkaloid alter the cytotoxic effect of its derivatives

This is the final peer-reviewed author's accepted manuscript (postprint) of the following publication:

Published Version:

Sabrina Burattini, M.B. (2022). Morpho-functional analyses reveal that changes in the chemical structure of a marine bisindole alkaloid alter the cytotoxic effect of its derivatives. *MICROSCOPY RESEARCH AND TECHNIQUE*, 86(7), 1-9 [10.1002/jemt.24092].

Availability:

This version is available at: <https://hdl.handle.net/11585/877804> since: 2022-03-08

Published:

DOI: <http://doi.org/10.1002/jemt.24092>

Terms of use:

Some rights reserved. The terms and conditions for the reuse of this version of the manuscript are specified in the publishing policy. For all terms of use and more information see the publisher's website.

This item was downloaded from IRIS Università di Bologna (<https://cris.unibo.it/>).
When citing, please refer to the published version.

(Article begins on next page)

1 **Changes in the chemical structure of the marine bisindole alkaloid 2,2-bis(6-bromo-1H-**
2 **indol-3-yl)ethanamine alter the cytotoxic effect of its derivatives**

3
4
5 Sabrina Burattini^{1a}, Michela Battistelli^{1a}, Michele Verboni¹, Elisabetta Falcieri¹, Simone Lucarini
6 ^{1*} and Sara Salucci ^{1,2*}

7
8 ¹Department of Biomolecular Sciences (DISB), University of Urbino Carlo Bo, 61029 Urbino,
9 Italy

10 ²Cellular Signalling Laboratory, Department of Biomedical and Neuro Motor Sciences
11 (DIBINEM), University of Bologna, 40126 Bologna, Italy

12
13 ^aequally contributed

14
15
16 Corresponding authors:
17 Dr. Sara Salucci, Department of Biomolecular Sciences, University of Urbino, via Ca' Le Suore
18 2, 61029 Urbino and Cellular Signalling Laboratory, Department of Biomedical and Neuromotor
19 Sciences, University of Bologna, Bologna, Italy. Email: sara.salucci@uniurb.it;

20 sara.salucci@unibo.it

21 Dr. Simone Lucarini - Department of Biomolecular Sciences, University of Urbino Carlo Bo,
22 piazza del Rinascimento 6, 61029 Urbino (PU), Italy; orcid.org/0000-0002-3667-1207; Phone:
23 +390722303333; Email: simone.lucarini@uniurb.it

24

25 **Abstract**

26 2,2-bis(6-bromo-1*H*-indol-3-yl)ethanamine, a marine alkaloid, appeared a potential anticancer
27 agent against several tumor cell models thanks to the presence of a 3,3'-diindolylmethane scaffold.
28 Here, the modifications in its chemical structure into alkaloid-like derivatives, have been evaluated,
29 to investigate changes in its biological activities. Three derivatives have been considered and their
30 potential apoptotic action has been evaluated through morpho-functional analyses in a human
31 cancer cell line.

32 Apoptosis appears strongly decreased in the derivative compounds without the bromine units (**1**)
33 and in those where the bromine groups have been substituted with fluorine atoms (**2**). On the
34 contrary, the methylation of indole NH (**3**) does not alter the alkaloid apoptotic activity that occurs
35 through the involvement of an increased oxidative stress, leading to peroxidation events and
36 mitochondria dysfunctionality.

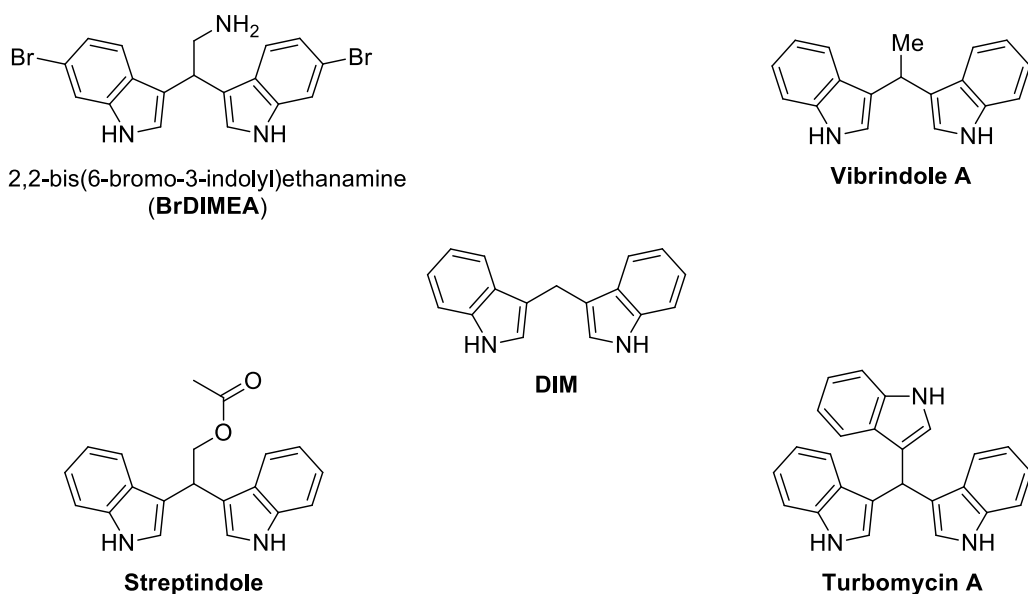
37 This manuscript highlights the alkaloid derivative cytotoxic effect, which is strictly correlated to
38 the maintenance of bisindole structure and bromine atoms. Since molecular therapies, by targeting
39 mitochondria pathways, have shown positive outcomes against several cancer cells, the alkaloid
40 with bisindole scaffold and the two bromine units can be considered a promising candidate to
41 develop new derivatives with strong anticancer property.

42
43 **Key words:** Marine alkaloids; bisindoles; structure-activity relationships, apoptotic activity;
44 mitochondria, anticancer activity, U937 **cell line**

45

46 **Introduction**

47 Marine bisindole alkaloids showed significant cytotoxicity, antineoplastic and antimicrobial
48 properties [1,2]. In particular, 2,2-bis(6-bromo-3-indolyl) ethanamine (**BrDIMEA**), isolated from
49 the Californian tunicate *Didemnum candidum* and the New Caledonian sponge *Orina* [3], is a
50 strong cytotoxic agent in various tumor cell lines [3-5]. In our previous paper, its apoptotic
51 mechanism of action, through caspase activation and regulated by Bcl-2 protein family, has been
52 demonstrated in U937 cells. For this potential anticancer activity, **BrDIMEA**, a member of the
53 large 3,3'-diindolylmethane family of alkaloids, has obtained much attention [3].



54
55 **Figure 1.** The marine alkaloid **BrDIMEA** and some natural antitumoral agents sharing the 3,3'-
56 diindolylmethane (**DIM**) scaffold.

57
58 Its anticancer properties are possibly due to the common 3,3'-diindolylmethane molecular unit
59 (**DIM**), a chemical group (Figure 1) which exhibit itself antiproliferative or apoptotic activities [6-
60 9]. The use of DIM is limited for lipophilic nature and *in vivo* chemical instability and it seems that
61 the presence of the alkylamino side chain improves its chemical and therapeutic activities [4]. In
62 addition, the presence of two bromoindole units could enhance the anti-cancer action. Therefore,

63 **BrDIMEA** can be considered a lead molecule for the synthesis of new compounds with a wide
64 range of biological properties, including the antineoplastic action.

65 In this study, the potential apoptotic effect of three different **BrDIMEA** derivatives (**1-3**), has been
66 evaluated through morpho-functional analyses on U937 human cancer cells by, comparing their
67 action with that of the natural compound.

68

69 **Materials and Methods**

70

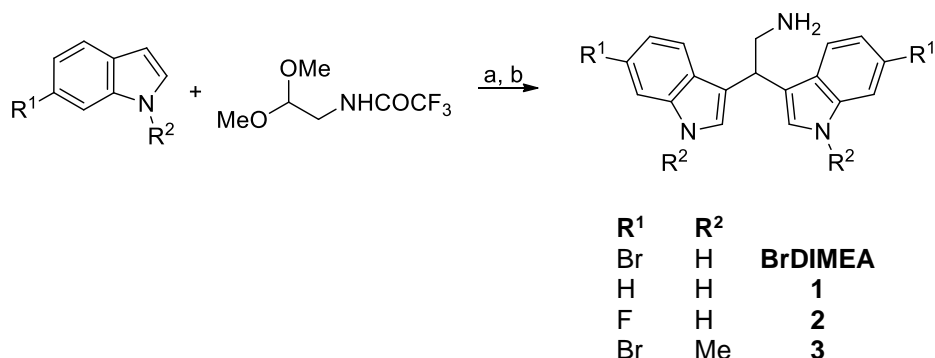
71 *Chemicals*

72 All organic solvents used in this study were purchased from Sigma–Aldrich (St. Louis, MO, USA),
73 Alfa Aesar (Haverhill, MA, USA), or TCI (Tokyo, Japan). Prior to use, acetonitrile,
74 dichloromethane and toluene were dried with molecular sieves with an effective pore diameter of
75 4 Å. Column chromatography purifications were performed under “flash” conditions using Merck
76 (Darmstadt, Germany) 230–400 mesh silica gel. Analytical thin-layer chromatography (TLC) was
77 carried out on Merck silica gel plates (silica gel 60 F254), which were visualized by exposure to
78 ultraviolet light and an aqueous solution of cerium ammonium molybdate (CAM). ESI-MS spectra
79 were recorded with a Waters (Milford, MA, USA) Micromass ZQ spectrometer. ¹H NMR and ¹³C
80 NMR spectra were recorded on a Bruker (Billerica, MA, USA) AC 400 or 100, respectively,
81 spectrometer and analyzed using the TopSpin 1.3 (2013) software package. Chemical shifts were
82 measured by using the central peak of the solvent. The final compounds were analyzed on a
83 ThermoQuest (Italia) FlashEA 1112 elemental analyzer for C, H, and N. The percentages found
84 were within ±0.4% of the theoretical values. All the tested compounds were >95% pure as
85 determined by elemental analysis.

86

87 *Chemistry*

88 Marine bisindole alkaloid **BrDIMEA** and compounds **1-3** were prepared as described in Scheme
89 1.



92 **Scheme 1.** Reaction conditions: (a) diphenyl phosphate, acetonitrile, 80°C, 24 h; (b) K₂CO₃,
93 methanol, reflux, 2 h.

94

95 *General procedure for the synthesis of derivatives **BrDIMEA** and **1-3***

96 Diphenyl phosphate (0.02 mmol) was added to a solution of the appropriate indole derivative (0.4
97 mmol) and (trifluoroacetyl amino)acetaldehyde dimethyl acetal (0.2 mmol) in anhydrous
98 acetonitrile (0.2 mL), and the resulting mixture was stirred at 80 °C for 24 h in a sealed tube,
99 monitoring the progress of the reaction by TLC and HPLC-MS. After cooling to room temperature,
100 saturated aqueous NaHCO₃ (30 mL) and dichloromethane (30 mL) were added and the two phases
101 were separated. The aqueous solution was extracted with dichloromethane (3 x 20 mL). After
102 drying over dry Na₂SO₄, the combined organic phases were concentrated in vacuum and the
103 resulting crude product was utilized without further purification. A mixture of that crude
104 trifluoroacetamide derivative and potassium carbonate (1 mmol) in MeOH (1.87 mL) and H₂O
105 (0.13 mL) was stirred and heated at reflux for 2 h. The MeOH was removed under reduced pressure
106 and water was added (30 mL). The aqueous solution was extracted with dichloromethane (3 x 30

107 mL) and the resulting solution was dried with Na₂SO₄ and concentrated in vacuum. The crude
108 material was purified by flash chromatography on neutral alumina.

109 The physico-chemical data of **BrDIMEA** [4,10] and **1-3** are in agreement with those reported.

110
111 **Cell Culture**
112 U937 human myelomonocytic lymphoma cell line, grown in RPMI 1640, supplemented with 10%
113 heat-inactivated fetal bovine serum, 2 mM glutamine, 1% antibiotics, was maintained at 37°C in
114 humidified air with 5% CO₂ [11]. Cell behavior was monitored with the Inverted Microscopy (IM;
115 Eclipse TE2000-S Nikon; objective 10x).

116
117 **Apoptosis induction**
118 U937 cells have been exposed to **BrDIMEA** and its derivatives **1-3**, at the final concentration in
119 the cell medium of 7.5 µM. This latter is the better apoptotic dose of **BrDIMEA**, already
120 demonstrated by Salucci et al., 2018 [3].

121 For apoptosis induction, cells (seeded at 1x10⁶ cells/mL) were exposed to three derivatives and to
122 **BrDIMEA**.

123 Trypan Blue (TB) exclusion assay [12] has been used to evaluate living and dead cells in control
124 condition and in treated samples.

125
126 **Transmission Electron Microscopy (TEM)**

127 U937 pellets were immediately fixed in 2.5% glutaraldehyde in 0.1 M in phosphate buffer, post-
128 fixed in 1% OsO₄ in the same buffer, dehydrated with ethanol and embedded in araldite [13].
129 Semithin sections have been counterstained with Blue of Toluidine and observed at light
130 microscope (LM). Thin sections, collected on nickel grids and stained with uranyl acetate and lead

131 citrate, were observed with an electron microscope (Philips CM10, 80KV, FEI Company, Italy).

132

133 **Confocal Laser Scanning Microscopy (CLSM)**

134 *TUNEL*

135 Control and treated cells were fixed with 4% paraformaldehyde in phosphate buffer saline (PBS)

136 pH 7.4 for 30 min., then deposited on poly-lysinated coverslips in Petri dishes overnight at 4 °C.

137 After PBS washing, samples were permeabilized with a 2:1 mixture of ethanol and acetic acid for

138 5 min at -20 °C. For the TUNEL technique, all reagents were part of the Apoptag Plus kit (D.B.A.,

139 Oncor, Dallas, TX, USA) and procedures were carried out according to the manufacturer's

140 instructions and as described in Salucci et al., 2014 [14]. Finally, slides were mounted with an

141 antifading medium. Specimens were observed with a Leica TCS-SP5 confocal laser scanning

142 microscope (CLSM) connected to a DMI 6000 CS inverted microscope (Leica Microsystems CMS

143 GmbH, Mannheim, Germany); excitation was at 488 nm and emission signals were detected at 517

144 nm.

145

146 *Mitochondrial behavior*

147 To monitor mitochondrial behavior, fresh cells were treated with 10 nonyl-acridine orange (NAO)

148 for evaluating mitochondria membrane integrity through peroxidation event evaluation. Fresh cells

149 were exposed to 50 nM NAO for 10 min at room temperature and then observed through a Leica

150 TCS-SP5 Confocal connected to a DMI 6000 CS Inverted Microscope (Leica Microsystems CMS

151 GmbH; objectives 40x and 60x).

152 Excitation was at 488nm (FITC and NAO); emission signals were detected at 525 nm (FITC) and

153 519 nm (NAO). CLSM images are presented as single-plane images or Z-stack projections [15].

154

155 **Results**

156 In the previous paper, the best **BrDIMEA** apoptotic action has been demonstrated in U937 cells at
157 the dose of 7.5 μ M.

158 In this work the effect of its derivatives, which show some modifications in their chemical
159 structures respect to the original alkaloid, has been analyzed. First of all, the ability of these
160 compounds to induce cytotoxicity in the same cell line has been evaluated through TB assay and the
161 number of living cells, expressed as mean value percentage \pm standard deviation, has been
162 calculated. Figure 2 shows micrographs obtained after IM and LM observations which revealed
163 living and dead cells in all experimental conditions together with a graph on cell viability
164 percentage. A good cell preservation confirmed by a high living cell number appears in control
165 condition (Fig. 2A, B). Cells treated with compound **1** or **2** (in which bromide atoms are deleted
166 and in the second compound substituted with the fluorine ones), show, at IM (Fig. 2C, E) or LM
167 (Fig. 2D, F), a morphological behavior similar to that observed in control condition. In both
168 situations, a reduction of cell viability about 10% has been quantified. On the other hand, the
169 compound **3**, which maintains the DID molecular unit and the bromide groups and in which two
170 hydrogen atoms from indole have been deleted, induces a diffuse presence of dead cells (Fig. 2G,
171 H). Therefore, the compound **3** causes a cytotoxic effect comparable to that observed after
172 **BrDIMEA** treatment in our previous work [3].

173 Morphological observations allow to distinguish the type of death and have been carried out for
174 the compound **3** alone. Compared to control cells, which show a preserved ultrastructure (Fig. 3A,
175 B), those exposed to 7.5 μ M compound **3**, became apoptotic and, in particular, late apoptotic events
176 can be observed (Fig. 3C, D). Therefore, an evident cell shrinkage, cytoplasmic vacuolization,
177 mitochondria damage, chromatin condensation, micronuclei and, sometimes, secondary necrosis
178 appear. Since compound **3** induces an apoptotic phenotype in U937 cells, the *in situ* DNA

179 fragmentation has been investigated, and the presence of a diffuse number of TUNEL positive
180 nuclei (Fig. 3 inset D), absent in control condition (Fig. 3 inset A) has been observed. In particular,
181 the fluorescent staining is localized inside micronuclei (Fig. 3 inset D).

182 For what concerns derivative **3**, the mitochondrial behavior has been also investigated. In
183 particular, the presence of cardiolipin peroxidation events have been analyzed with the fluorescent
184 probe NAO at CLSM. Respect to control cells, in which mitochondrial membrane maintains its
185 integrity (Fig. 3E, F), those treated with compound **3** show a decline of fluorescence intensity (Fig.
186 3G, H) suggesting that the loss of mitochondrial membrane integrity could favor the release of pro-
187 apoptotic proteins from the mitochondria. This latter result confirms the ultrastructural
188 observations, in fact cells treated with compound **3** showed dysfunctional mitochondria which
189 appear empty or with altered cristae, a typical condition induced by an increased oxidative stress.

190

191 **Discussion**

192 Apoptosis is a programmed cell death which maintains the healthy survival/death balance in cells
193 [16,17]. Misregulation of apoptosis can cause cancer or autoimmunity, while enhanced apoptosis
194 may cause degenerative diseases [11,18]. Researchers are involved in the development of some
195 promising cancer treatment strategies which target apoptotic inhibitors including Bcl-2 family
196 proteins and other substrates. One strong apoptotic agent in various cell models appears a marine
197 bisindole alkaloid [19,20], which induces apoptosis in U937 cells following both extrinsic and
198 intrinsic pathways and by involving the Bcl-2 protein family. In particular, Salucci and
199 collaborators demonstrated the ability of this chemical alkaloid to up-regulate bax and to inactivate
200 Bcl-2 and Bcl-xL [3], the anti-apoptotic factors, which block the release of cytochrome c from
201 mitochondria and thus promote cell survival. Since the 2,2-bis(6-bromo-3-indolyl)-ethanamine
202 targets anti-apoptotic Bcl-2 protein and, consequently, can have success in killing many types of

203 cancer, its chemical structure can be considered the basic scaffold to obtain synthetic derivatives
204 with similar biological properties but with an improved chemical stability [21].
205 For that, in this study, we have evaluated the anti-cancer potential action of three bisindole alkaloid
206 derivatives. To identify and confirm the chemical unit responsible of apoptotic effect, a preliminary
207 structure-activity relationships of 2,2-bis(6-bromo-3-indolyl)-ethanamine have been carried out.
208 Morpho-functional analyses revealed that, in the same cell model and at the same dosage, only the
209 compound **3** maintains an apoptotic effect similar to that observed after **BrDIMEA**. Moreover,
210 compound **3** is able to induce apoptotic cell death through the oligonucleosomic DNA cleavage
211 and by involving the mitochondrial pathway. In fact, mitochondrial membrane integrity appears
212 loss due to cardiolipin peroxidation, which leads to the formation of reactive aldehydes, able to
213 react with proteins and DNA [22]. Ultrastructural analyses reveal the presence of a high number of
214 empty mitochondria suggestive of oxidative stress increase. This data enhances that oxidative stress
215 production can be considered one of the major causes of apoptosis in cancer cells and it could be
216 recognized into a promising therapeutic approach for the cancer treatment [23].
217 These findings show that the **BrDIMEA** derivative **3** induces apoptosis via mitochondrial pathway
218 and with a rate similar to that observed for the marine alkaloid lead compound, demonstrating that
219 the bisindole scaffold, even N-methylated, as well as the bromine atoms, are necessary and must
220 be maintained for developing new anticancer drug.

221

222

223 **Acknowledgments:** This work has been possible thanks to the DISB 2017 Enhancement Project
224 of Urbino University.

225

226 **Author Contributions:**

227 Methodology, S.B.,M.B., S.L.,S.S; Investigation, S.S.; Data Curation, S.S. and S.L.; Writing –
228 Original Draft Preparation, S.S and S.L.; Writing – Review & Editing, S.S and S.L.; Supervision,
229 S.L. and S.S.

230 **References**

- 231 1. Veale, C.G.; Davies-Coleman, M.T. Chapter one: Marine Bi-, Bis-, and Trisindole Alkaloids.
232 *In: Alkaloids Chem Biol, Elsevier* **2014**, 73, 1- 64.
- 233 2. Kamel, M.M.; Abdel-Hameid, M.K.; El-Nassan, H.B.; El-Khouly, E.A. Synthesis and Cytotoxic
234 Activity of Novel Mono- and Bis-Indole Derivatives: Analogues of Marine Alkaloid
235 Nortopsentin. *Med Chem.* **2020**, 17, 779-789.
- 236 3. Salucci, S.; Burattini, S.; Buontempo, F.; Orsini, E.; Furiassi, L.; Mari, M.; Lucarini, S.;
237 Martelli, A.M.; Falcieri, E. Marine bisindole alkaloid: A potential apoptotic inducer in human
238 cancer cells. *Eur J Histochem.* **2018**, 62, 2881.
- 239 4. Mari, M.; Tassoni, A.; Lucarini, S.; Fanelli, M.; Piersanti, G.; Spadoni, G. Brønsted Acid
240 Catalyzed Bisindolization of α -Amido Acetals: Synthesis and Anticancer Activity of
241 Bis(indolyl)ethanamino Derivatives. *Eur J Org Chem.* **2014**, 2014, 3822-3830.
- 242 5. Mantenuto, S.; Lucarini, S.; De Santi, M.; Piersanti, G.; Brandi, G.; Favi, G. One-Pot Synthesis
243 of Biheterocycles Based on Indole and Azole Scaffolds Using Tryptamines and 1,2-Diaza-1,3-
244 dienes as Building Blocks. *Eur J Org Chem.* **2016**, 2016, 3193-3199.
- 245 6. Junaid, M.; Dash, R.; Islam, N.; Chowdhury, J.; Alam, M.J.; Nath, S.D.; Shakil, M.A.S.; Azam,
246 A.; Quader, S.M.; Zahid Hosen, S.M. Molecular Simulation Studies of 3,3'-Diindolylmethane
247 as a Potent MicroRNA-21 Antagonist. *J Pharm Bioallied Sci.* **2017**, 9, 259-265.
- 248 7. Tian, X.; Liu, K.; Zu, X.; Ma, F.; Li, Z.; Lee, M.; Chen, H.; Li, Y.; Zhao, Y.; Liu, F.; Oi, N.;
249 Bode, A.M.; Dong, Z.; Kim, D.J. 3,3'-Diindolylmethane inhibits patient-derived xenograft colon
250 tumor growth by targeting COX1/2 and ERK1/2. *Cancer Lett.* **2019**, 448, 20-30.
- 251 8. Lanza-Jacoby, S.; Cheng, G. 3,3'-Diindolylmethane enhances apoptosis in docetaxel-treated
252 breast cancer cells by generation of reactive oxygen species. *Pharm Biol.* **2018**, 56, 407-414.
- 253 9. Condello, M.; Pellegrini, E.; Multari, G.; Gallo, F.R.; Meschini, S. Voacamine: Alkaloid with

- 254 its essential dimeric units to reverse tumor multidrug resistance. *Toxicol In Vitro*. **2020**, *65*,
255 104819.
- 256 10. Campana, R.; Favi, G.; Baffone, W.; Lucarini, S. Marine Alkaloid 2,2-Bis(6-bromo-3-indolyl)
257 Ethylamine and Its Synthetic Derivatives Inhibit Microbial Biofilms Formation and
258 Disaggregate Developed Biofilms. *Microorganisms* 2019, *7*, 28.
- 259 11. Salucci, S.; Battistelli, M.; Burattini, S.; Sbrana, F.; Falcieri E. Holotomographic microscopy:
260 A new approach to detect apoptotic cell features. *Microsc Res Tech*. **2020**, *83*, 1464-1470.
- 261 12. Salucci, S.; Burattini, S.; Giordano, F.M.; Diamantini, G.; Falcieri, E. Further highlighting on
262 the prevention of oxidative damage by polyphenol-rich wine extracts. *J Med Food*, **2017**, *20*,
263 410-419.
- 264 13. Giordano, F.M.; Burattini, S.; Buontempo, F.; Canonico, B.; Martelli, A.M.; Papa, S.;
265 Sampaolesi, M.; Falcieri, E.; Salucci, S. Diet Modulation Restores Autophagic Flux in Damaged
266 Skeletal Muscle Cells. *J Nutr Health Aging*. **2019**, *23*, 739-745.
- 267 14. Salucci, S.; Burattini, S.; Battistelli, M.; Baldassarri, V.; Curzi, D.; Valmori, A.; Falcieri, E.
268 Melatonin prevents chemical-induced haemopoietic cell death. *Int J Mol Sci*. **2014a**, *15*, 6625-
269 6640.
- 270 15. Salucci, S.; Battistelli, M.; Baldassarri, V.; Burini, D.; Falcieri, E.; Burattini, S. Melatonin
271 prevents mitochondrial dysfunctions and death in differentiated skeletal muscle cells. *Microsc*
272 *Res Tech*. **2017**, *80*, 1174-1181.
- 273 16. Salucci, S.; Burattini, S.; Curzi, D.; Buontempo, F.; Martelli, A.M.; Zappia, G.; Falcieri, E.;
274 Battistelli, M. Antioxidants in the prevention of UVB-induced keratynocyte apoptosis. *J*
275 *Photochem Photobiol B*. **2014b**, *141*, 1-9.
- 276 17. Voss, A.K.; Strasser, A. The essentials of developmental apoptosis. *F1000Res*. **2020**, *9*, F1000
277 Faculty Rev-148.

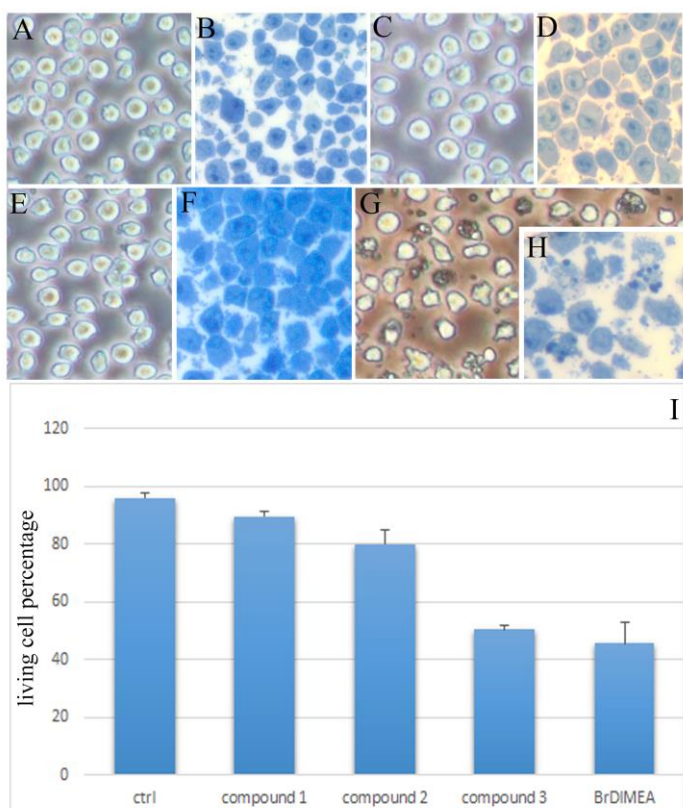
- 278 18. Carneiro, B.A.; El-Deiry, W.S. Targeting apoptosis in cancer therapy. *Nat Rev Clin Oncol.*
279 **2020**, *17*, 395-417.
- 280 19. Zhang, Y.; Hu, C. Anticancer activity of bisindole alkaloids derived from natural sources and
281 synthetic bisindole hybrids. *Arch Pharm (Weinheim)*. **2020**, *353*, e2000092.
- 282 20. Lunagariya, J.; Bhadja, P.; Zhong, S.; Vekariya, R.; Xu, S. Marine Natural Product Bis-indole
283 Alkaloid Caulerpin: Chemistry and Biology. *Mini Rev Med Chem*. **2019**, *19*, 751-761.
- 284 21. Imran, S.; Taha, M. Ismail, N.H. A Review of Bisindolylmethane as an Important Scaffold for
285 Drug Discovery. *Curr Med Chem*. **2015**, *22*, 4412-4433.
- 286 22. Pizzimenti, S.; Toaldo, C.; Pettazzoni, P., Dianzani, M.U.; Barrera, G. The "two-faced" effects
287 of reactive oxygen species and the lipid peroxidation product 4-hydroxynonenal in the hallmarks
288 of cancer. *Cancers (Basel)*. **2010**, *2*, 338-363.
- 289 23. Barrera, G.; Gentile, F.; Pizzimenti, S.; Canuto, R.A.; Daga, M.; Arcaro, A.; Cetrangolo, G.P.;
290 Lepore, A.; Ferretti, C.; Dianzani, C.; Muzio, G. Mitochondrial Dysfunction in Cancer and
291 Neurodegenerative Diseases: Spotlight on Fatty Acid Oxidation and Lipoperoxidation Products.
292 *Antioxidants (Basel)*. **2016**, *5*, 7.

293

294

295 **Figure legends**

296



297

298

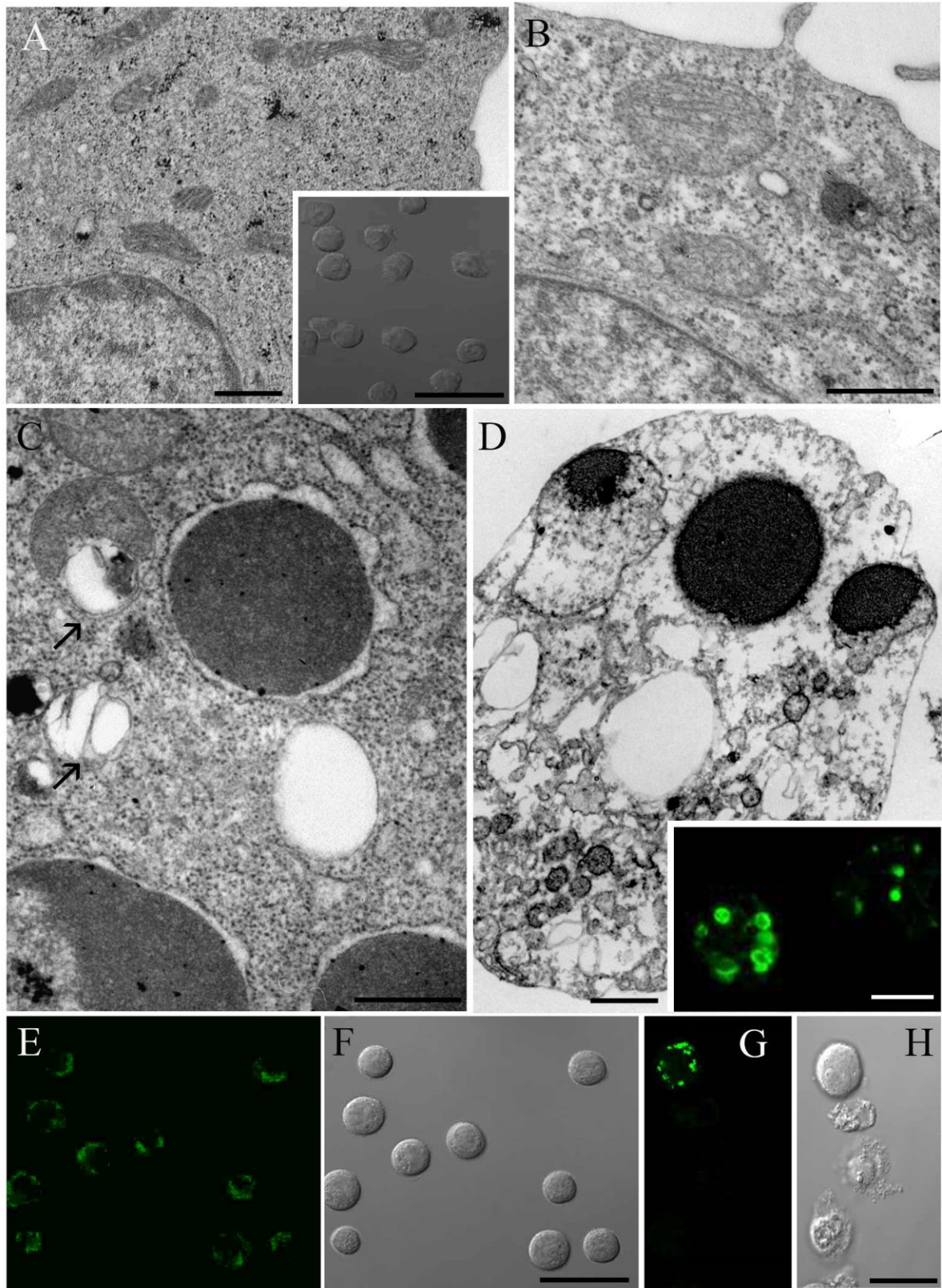
299 **Figure 2. IM and LM observations of control condition (A, B) and BrDIMEA derivative 1 (C,**

300 **D), 2 (E, F) 3 (G, H) treated cells.** The graph in I shows TB exclusion assay which reveals a cell

301 viability reduction after drug administration. Data are from three separate experiments and

302 furnished as mean +/- standard deviation. Bars: 10 μ m

303



305
306 **Figure 3. TEM (A-D) and CLSM observations (inset A and C, E-H) of control cells (A, inset**
307 **A, B, E, F) and those exposed to compound 3 (C, D, inset D, G, H).** Apoptotic features, altered
308 mitochondria (arrows) and TUNEL positive nuclei, absent in control condition (A, B and inset A)
309 appears after compound 3 administration (C, D, inset D). If control cells maintain the mitochondrial
310 membrane integrity (E, F), treated cells (G, H) show a decrease of fluorescence after NAO staining
311 evidencing the presence of peroxidation events. Bars: 500nm for A-D; 5 μ m for inset D; 10 μ m
312 for inset A, E-H.

313

314

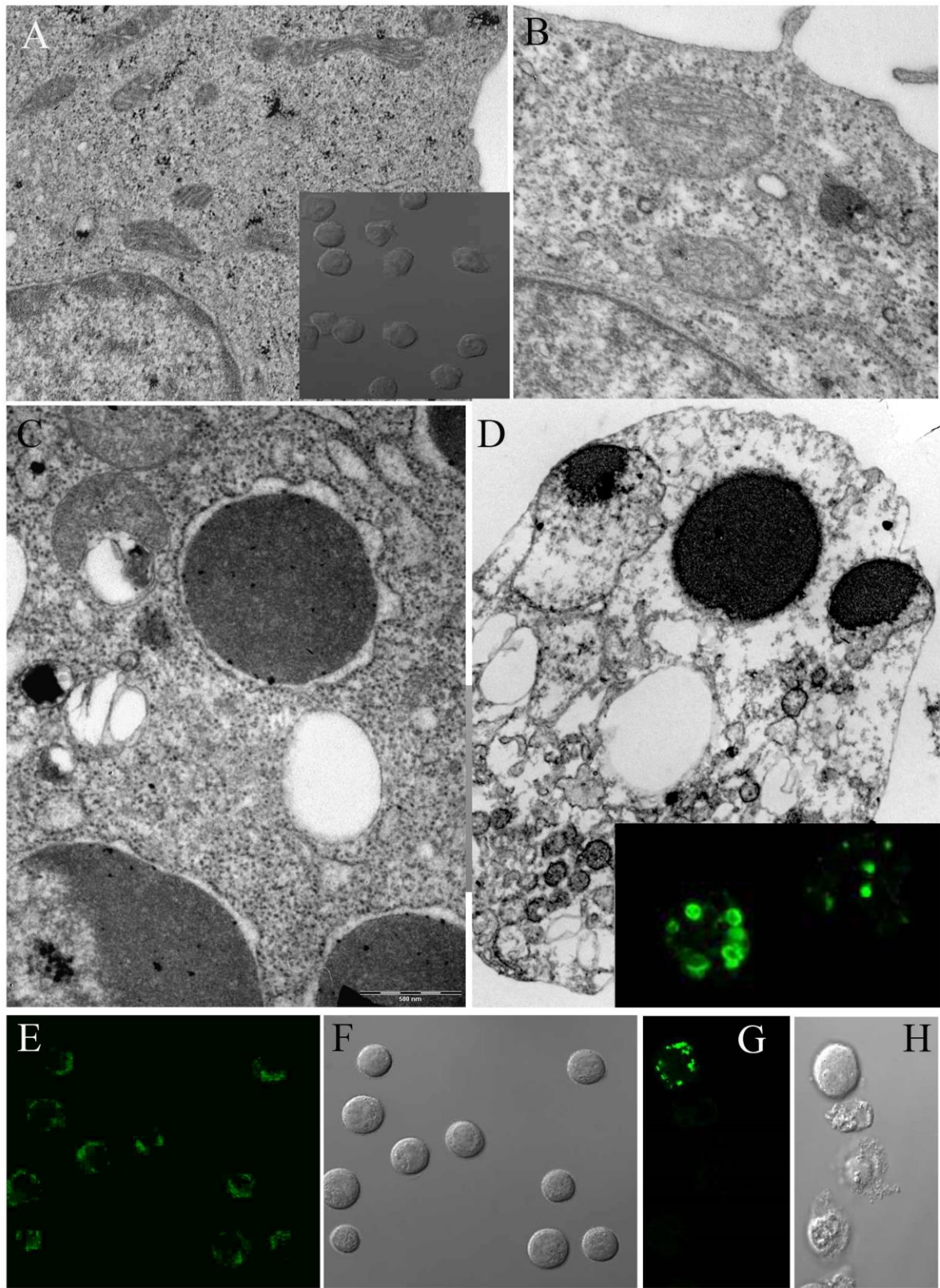
315

316

317

318

319



320

321 **Fig. 3**